

## ORIGINAL ARTICLE

# Stimulation of osteoclast migration and bone resorption by C–C chemokine ligands 19 and 21

Jiyeon Lee<sup>1</sup>, Cheolkyu Park<sup>1</sup>, Hyung Joon Kim<sup>1</sup>, Yong Deok Lee<sup>1</sup>, Zang Hee Lee<sup>1</sup>, Yeong Wook Song<sup>2,3</sup> and Hong-Hee Kim<sup>1</sup>

Osteoclasts are responsible for the bone erosion associated with rheumatoid arthritis (RA). The upregulation of the chemokines CCL19 and CCL21 and their receptor CCR7 has been linked to RA pathogenesis. The purpose of this study was to evaluate the effects of CCL19 and CCL21 on osteoclasts and to reveal their underlying mechanisms. The expression of CCL19, CCL21 and CCR7 was higher in RA patients than in osteoarthritis patients. In differentiating osteoclasts, tumor necrosis factor- $\alpha$ , interleukin-1 $\beta$  and lipopolysaccharide stimulated CCR7 expression. CCL19 and CCL21 promoted osteoclast migration and resorption activity. These effects were dependent on the presence of CCR7 and abolished by the inhibition of the Rho signaling pathway. CCL19 and CCL21 promoted bone resorption by osteoclasts in an *in vivo* mice calvarial model. These findings demonstrate for the first time that CCL19, CCL21 and CCR7 play important roles in bone destruction by increasing osteoclast migration and resorption activity. This study also suggests that the interaction of CCL19 and CCL21 with CCR7 is an effective strategic focus in developing therapeutics for alleviating inflammatory bone destruction.

*Experimental & Molecular Medicine* (2017) 49, e358; doi:10.1038/emm.2017.100; published online 21 July 2017

## INTRODUCTION

Rheumatoid arthritis (RA) is an autoimmune disease that causes inflammation and bone destruction in joint areas. Bone destruction by osteoclasts becomes more severe as the disease progresses.<sup>1</sup> Osteoclast precursors (monocytes and macrophages) and osteoclasts are recruited to the inflamed synovium and are activated to evoke the erosion of subchondral bone.<sup>2</sup> Therefore, the migration of these cells to joint areas is an important step in RA pathogenesis. Several factors, such as CXCL12 (SDF-1), TGF- $\beta$  and CX<sub>3</sub>CL1 (fractalkine), have been reported to promote osteoclast migration.<sup>3–5</sup> These factors enhance osteoclast recruitment to the bone surface and in some cases augment osteoclastogenesis directly or indirectly.

The chemokines CCL19 and CCL21 both recruit various types of cells, such as leukocytes, immune cells and certain tumor cells.<sup>6–11</sup> In particular, both CCL19 and CCL21 promote the *in vitro* migration and maturation of dendritic cells, which share their precursors with osteoclasts.<sup>12,13</sup> In mice, the genetic deletion of CCR7, the receptor shared by CCL19 and CCL21, led to a loss of dendritic cell migration ability.<sup>14</sup> In addition,

the localization of macrophages in the marginal zone of the spleen is regulated by CCL19 and CCL21.<sup>15</sup> These reports suggest that CCL19 and CCL21 are involved in the migration and/or activation of osteoclasts.

CCR7 is a G-protein-linked cell-surface receptor that is expressed in hematopoietic cells, such as T cells, B cells, dendritic cells, macrophages and neutrophils.<sup>16</sup> The common function of CCR7 in these cells is the promotion of migration. A recent study reported that via CCR7, CCL19 stimulates the migration of bone marrow mesenchymal stem cells that can differentiate into osteoblasts.<sup>17</sup> However, the function of CCR7 in osteoclasts has not yet been investigated.

Recent studies have shown that the expression of CCL19 and CCL21 is elevated in the synovial tissues of RA patients.<sup>18</sup> An investigation revealed that the levels of CCL19 in plasma and the CCR7 expression on monocytes increased in early RA conditions; these were decreased by 1 year and 5 years of RA therapy.<sup>19</sup> These results suggest that CCL19 and CCL21 and their receptor CCR7 might be crucial for RA pathophysiology.

<sup>1</sup>Department of Cell and Developmental Biology, BK21 Program and Dental Research Institute, Seoul National University, Seoul, Korea; <sup>2</sup>Department of Molecular Medicine and Biopharmaceutical Sciences, Graduate School of Convergence Science and Technology, and College of Medicine, Seoul National University, Seoul, Korea and <sup>3</sup>Division of Rheumatology, Department of Internal Medicine, College of Medicine, Seoul National University, Seoul, Korea  
Correspondence: Professor H-H Kim, Department of Cell and Developmental Biology, BK21 Program and Dental Research Institute, Seoul National University, 28 Yongeon-Dong, Chongno-Ku, Seoul 03080, Korea.

E-mail: hhbkim@snu.ac.kr

Received 12 September 2016; revised 22 January 2017; accepted 31 January 2017

The intracellular signaling pathways triggered by CCR7 have not been well described. However, the small GTPase protein RhoA is suggested to be responsible for the CCR7-dependent migration of monocytes.<sup>20</sup> In addition, CCR7-mediated chemotaxis and the polarization of T cells were shown to require Rho kinase (ROCK), a downstream target of RhoA.<sup>21</sup> RhoA and other small GTPase family proteins are also reported to stimulate cytoskeleton rearrangement, migration, and the bone resorption activity of osteoclasts.<sup>22–24</sup> Therefore, CCR7 and its ligands may play important roles in the migration of osteoclasts via RhoA and ROCK.

In this study, we investigated the effects of CCL19 and CCL21 on osteoclast migration and bone resorption. The underlying mechanisms by which these chemokines function in osteoclasts were also explored.

## MATERIALS AND METHODS

### Reagents

Recombinant CCL19 and CCL21 were obtained from Prospec (East Brunswick, NJ, USA). The primary antibodies for CCR7, phosphoSer19 MLC (p-MLC) and  $\beta$ -actin were purchased from Abcam (Cambridge, Cambridgeshire, UK), Millipore (Temecula, CA, USA) and Sigma (St Louis, MO, USA), respectively. The antimouse and antirabbit secondary antibodies and Rho inhibitors simvastatin and Y27632 were obtained from Sigma. The Rho Activation Assay kits were bought from Millipore. CCR7 small interference RNA (siRNA) was provided by Santa Cruz Biotechnology (Santa Cruz, CA, USA). The siRNA transfection reagent HiPerFect was obtained from Qiagen (Valencia, CA, USA).

### Osteoclast differentiation

Murine osteoclast differentiation culturing was performed as previously described.<sup>25</sup> Bone marrow cells were flushed from the femurs and tibias of 5-week-old female ICR mice. Harvested cells were incubated in culture dishes for 1 day, and nonadherent cells were incubated further in Petri dishes with M-CSF (30 ng ml<sup>-1</sup>). After 3 days of culture, the adherent cells were collected and considered to be bone marrow-derived macrophages (BMMs). The BMMs were cultured in  $\alpha$ -MEM containing 10% FBS with M-CSF (30 ng ml<sup>-1</sup>) and RANKL (100 ng ml<sup>-1</sup>) for osteoclast differentiation.

### Enzyme-linked immunosorbent assay

The CCL19 and CCL21 levels were measured using CCL19 and CCL21 enzyme-linked immunosorbent assay (ELISA) kits following the manufacturer's instructions (R&D Systems, Minneapolis, MN, USA). To prepare the ELISA plates, the capture antibodies were diluted in PBS to a working concentration. A volume of 100  $\mu$ l of the antibodies was added to 96-well plates, and the plates were incubated overnight at room temperature. The wells were aspirated and washed with wash buffer three times. The plates were blocked with 300  $\mu$ l of diluent reagent, incubated for 1 h at room temperature, and washed again. A volume of 100  $\mu$ l of standards or samples diluted in diluent reagent was prepared. The samples were added to the wells and incubated for 2 h at room temperature. The plates were washed with wash buffer. After adding 100  $\mu$ l of the detection antibodies to the wells, the plates were incubated for 2 h at room temperature and washed with wash buffer. A volume of 100  $\mu$ l of streptavidin-HRP reagent was added to the wells, and the plates were incubated for 20 min at room temperature without direct light. After washing three

times, 100  $\mu$ l of substrate solution was added to the wells, and the plates were incubated for 20 min at room temperature without direct light. Stop solution (50  $\mu$ l) was added, and the optical density of the wells was measured immediately at 450 nm. The sera and synovial fluids were from osteoarthritis (OA) ( $n = 15$ ) and RA ( $n = 24$ ) patients. Patient samples were handled following the guidelines of the Institutional Review Board of Seoul National University Hospital.

### Real-time PCR

The total RNA was isolated using TRIzol (Invitrogen, Carlsbad, CA, USA) and reverse-transcribed using SuperScript II reverse transcriptase (Invitrogen). Complementary DNA was amplified with primers using a real-time PCR instrument (AB7500, Life Technologies, Carlsbad, CA, USA). The expression of mRNA was normalized to the 18S rRNA gene.

### Western blot analysis

The cells were lysed with 6  $\times$  boiling SDS sample buffer. The protein samples were quantified using protein assay kits (Bio-Rad, Hercules, CA, USA), and 30  $\mu$ g were loaded onto polyacrylamide gels. The separated proteins were transferred to nitrocellulose membranes. The membranes were blocked in 5% skim milk followed by incubation with the primary antibody (1:1000) overnight at 4  $^{\circ}$ C and the secondary antibody (1:10 000) for 1 h at room temperature. Immunoreactive bands were detected with chemiluminescence reagents.

### TRAP staining

BMMs were seeded at  $2 \times 10^4$  cells per well and cultured under differentiation conditions. After 4 days, the cells were fixed with 3.7% formaldehyde for 15 min and permeabilized with 0.1% Triton X-100 for 1 min. The cells were treated with tartrate-resistant acid phosphatase (TRAP) staining solution (Sigma) following the manufacturer's protocol. After 15 min, the TRAP-positive cells were counted under an Olympus 23 light microscope (Olympus, Tokyo, Japan).

### Flow cytometry

BMMs were incubated with lipopolysaccharide (LPS) (5 ng ml<sup>-1</sup>) for 1 day. The cells were collected with a scraper, washed by centrifugation at 400 g for 5 min for a total of three times in PBS containing 2% FBS, and incubated with the CCR7 antibody (1:40) for 30 min at 4  $^{\circ}$ C. After washing three more times, the cells were treated with a secondary antibody (1:1000) (Invitrogen) for 20 min and washed three times. Immediately, the cells were analyzed with a FACSCalibur flow cytometer (BD Science, Franklin Lakes, NJ, USA).

### Small interference RNA transfection

BMMs ( $2 \times 10^5$ ) were seeded in six-well culture plates and incubated for 24 h. Mixtures of 20 nmole siRNA oligonucleotides and the HiPerFect reagent were added to the wells. After 24 h, the medium was replaced with fresh medium, and the cells were cultured.

### Cell migration assays

The BMM migration assays used transwell migration assay kits (Corning, Corning, NY, USA). BMMs ( $1 \times 10^5$ ) were seeded in the upper chambers, and CCL19 or CCL21 was added to the lower chambers. For Rho inhibitor experiments, BMMs were pretreated with simvastatin or Y27632 for 1 h. After incubating for 18 h at 37  $^{\circ}$ C, the cells were fixed in 3.7% formaldehyde for 30 min and stained with crystal violet for 10 min. For the osteoclast migration experiments,

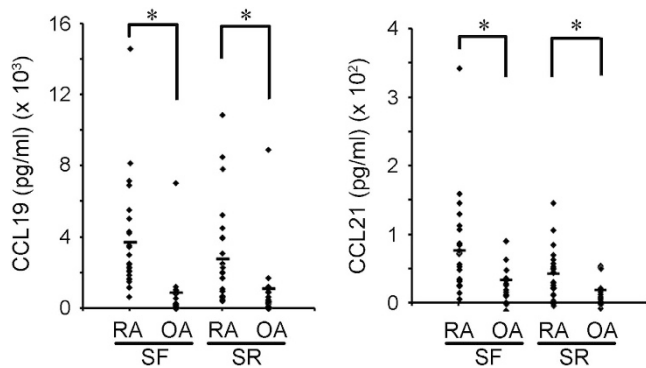


**Figure 1** Upregulation of CCL19 and CCL21 in RA patients. The levels of CCL19 and CCL21 in the synovial fluids and sera from RA ( $n=24$ ) and OA ( $n=15$ ) patients. The CCL19 and CCL21 levels were measured using human ELISA kits. OA, osteoarthritis; RA, rheumatoid arthritis.

Oris Cell Migration Assay kits (Platypus Technologies, Madison, WI, USA) were used. BMMs ( $1 \times 10^5$ ) were seeded in assay plates with stoppers and cultured in the presence of RANKL ( $100 \text{ ng ml}^{-1}$ ) and M-CSF ( $30 \text{ ng ml}^{-1}$ ). After 2 days, the stoppers were removed to allow the cells to migrate into the detection zone. After 16 h at  $37^\circ\text{C}$ , the cells were fixed with 3.7% formaldehyde and stained with crystal violet.

#### Rho pull-down assays

BMM cells ( $2 \times 10^6$ ) were cultured in 100-mm culture dishes and stimulated with CCL19 or CCL21 for the indicated times. The cells were harvested in lysis buffer (125 mM HEPES, pH 7.5, 570 mM NaCl, 5% Igepal CA-630, 50 mM  $\text{MgCl}_2$ , 5 mM EDTA and 10% glycerol) from the Rho Activation Assay kits. Protein samples were obtained from the cell extracts by centrifugation and incubated with 20  $\mu\text{l}$  of the Rho Assay Reagent slurry (beads) for 1 h at  $4^\circ\text{C}$ . The beads were washed three times in lysis buffer, and reducing sample buffer was added. After boiling, the samples were used for western blots.

#### Resorption assays

BMMs were seeded on calcium phosphate-coated plates and cultured with M-CSF ( $30 \text{ ng ml}^{-1}$ ) and RANKL ( $100 \text{ ng ml}^{-1}$ ) in the presence or absence of CCL19 ( $10 \text{ ng ml}^{-1}$ ) or CCL21 ( $10 \text{ ng ml}^{-1}$ ) for 6 days. After washing out the cells with distilled water, the plates were treated with a 5% silver nitrate solution for 1 h, washed with distilled water and treated with a sodium carbonate-formaldehyde solution (5%  $\text{Na}_2\text{CO}_3$ , 9.25% formaldehyde) for 2 min. Alternatively, BMMs were cultured on dentin slices with M-CSF ( $30 \text{ ng ml}^{-1}$ ) and RANKL ( $100 \text{ ng ml}^{-1}$ ) in the absence or presence of CCL19 ( $10 \text{ ng ml}^{-1}$ ) or CCL21 ( $10 \text{ ng ml}^{-1}$ ). After 6 days, the dentin slice surfaces were analyzed by confocal microscopy. The resorption pit areas were quantified after staining the dentin slices with Trypan Blue.

#### Confocal fluorescence microscopy

BMMs were cultured with M-CSF ( $30 \text{ ng ml}^{-1}$ ) and RANKL ( $100 \text{ ng ml}^{-1}$ ) with or without CCL19 ( $10 \text{ ng ml}^{-1}$ ) and CCL21 ( $10 \text{ ng ml}^{-1}$ ) for 6 days. The cells were fixed with 3.7% formaldehyde for 30 min, blocked in 1% bovine serum albumin for 2 h, and treated with phalloidin rhodamine for 2 h. The cells were washed with PBS containing 1% BSA three times after each step. The cell nuclei were

stained with 4,6-diamidino-2-phenylindole (DAPI). Zeiss LSM 7 PASCAL laser-scanning microscope (Carl Zeiss Microimaging, GmbH, Goettingen, Germany) was used to observe the actin rings.

#### *In vivo* mouse calvarial assay

Collagen sponges were soaked in 2  $\mu\text{g}$  of CCL19, CCL21 or PBS and transplanted into 5-week-old ICR mouse calvariae subcutaneously. For LPS injection experiments, LPS ( $1 \text{ mg kg}^{-1}$ ) was injected into 5-week-old ICR mice intraperitoneally twice at 4-day intervals with the first injection 1 day before CCL19 transplantation. The mice were killed 7 days after transplantation. The calvariae were collected, fixed in 4% paraformaldehyde for 1 day and analyzed by micro-computed tomography ( $\mu\text{-CT}$ ) using a SkyScan 1072 instrument (SkyScan, Aartselaar, Belgium). The calvariae from the CCL19- or CCL21-treated group and the control group were fixed in 4% paraformaldehyde for 18 h and decalcified with 12% EDTA for 4 weeks. The calvariae were dehydrated with 70–100% ethanol, cleared with chloroform and embedded in paraffin. The paraffin blocks were sectioned at 5  $\mu\text{m}$  thickness. Tissue sections were placed on slide glasses and stained with TRAP solution. Histomorphometric analyses were performed with the Osteomeasure program (OsteoMetrics, GA, USA). All animal experiments were reviewed and approved by the Institutional Animal Care and Use Committee of Seoul National University.

#### Statistical analysis

All experiments, except the human sample analyses and *in vivo* calvarial bone resorption assays, were performed at least three times. The quantitative data were expressed as the mean  $\pm$  s.d. *P*-values were determined by a two-tailed Student's *t*-test or a one-way analysis of variance followed by Tukey's test. *P*-values  $< 0.05$  were considered significant.

## RESULTS

### Expression of CCL19, CCL21 and CCR7 is elevated in RA patients

In the course of screening the chemokines differentially expressed in RA specimens compared to OA samples, we found that the protein levels of CCL19 and CCL21 were higher in the RA samples. The ELISA analyses showed a significantly higher level of those chemokines both in the synovial fluids and in the sera (Figure 1). Our results agree with previous reports from an immunostaining study of the synovial tissues and an ELISA study with the synovial fluids from RA patients.<sup>18</sup>

We also scrutinized microarray data deposited in the Gene Expression Omnibus (GEO, <http://www.ncbi.nlm.nih.gov/gds>) to gain further evidence of the link between CCL19 and CCL21 and RA. GEO data GPL91:GSE1919 showed that the mRNA of CCL19, but not CCL21, was more abundant in the synovial tissues of RA patients than in those of normal donors (Supplementary Figure 1). Although statistical significance was lacking, perhaps because of the small number of samples, there were higher levels of CCL19 and CCL21 mRNA in RA synovial tissues than in OA tissues (Supplementary Figure 1).

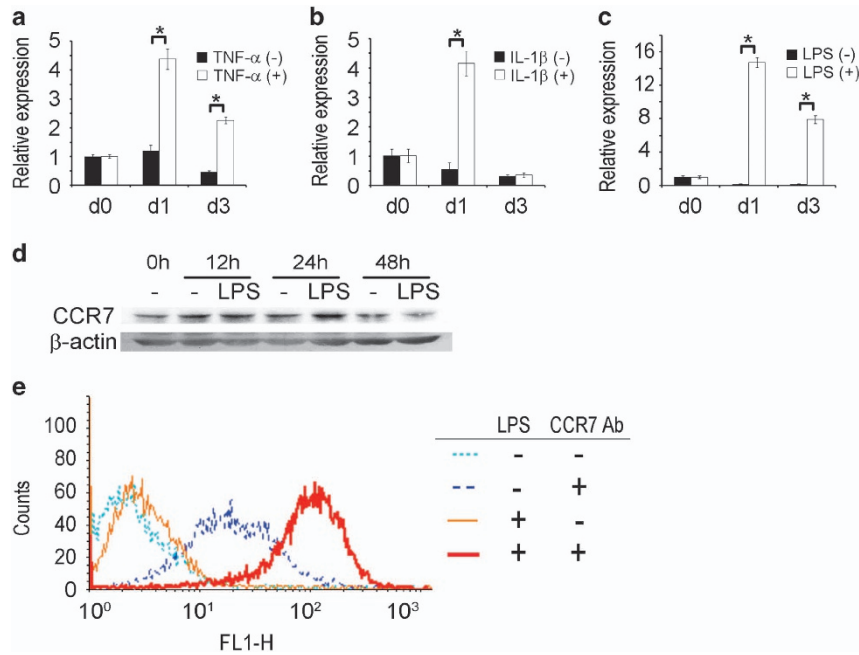


**Figure 2** Inflammatory stimuli increase CCR7 expression in BMMs and osteoclasts. (a–c) The CCR7 mRNA levels in BMMs treated with RANKL in the absence and presence of TNF- $\alpha$ , IL-1 $\beta$  and LPS. BMMs were treated with M-CSF (30 ng ml<sup>-1</sup>) and RANKL (100 ng ml<sup>-1</sup>) for 1 day or 3 days with concomitant TNF- $\alpha$  (5 ng ml<sup>-1</sup>), IL-1 $\beta$  (5 ng ml<sup>-1</sup>), LPS (5 ng ml<sup>-1</sup>) or control vehicle. The CCR7 mRNA was measured by real-time PCR. The internal control was the mRNA for 18S rRNA. (d) The CCR7 protein level in BMMs stimulated with LPS. BMMs were treated with LPS (5 ng ml<sup>-1</sup>) for 12, 24 and 48 h. The whole-cell lysates were used for western blotting.  $\beta$ -Actin was used as a loading control. (e) The cell-surface level of CCR7 protein in BMMs stimulated with LPS. BMMs were treated with LPS (5 ng ml<sup>-1</sup>) or PBS for 24 h. The cells were collected and subjected without permeabilization to flow cytometry with an anti-CCR7 antibody. The CCR7 antibody was omitted in the controls. BMM, bone marrow-derived macrophages; IL-1 $\beta$ , interleukin-1 $\beta$ ; LPS, lipopolysaccharide; OA, osteoarthritis; RA, rheumatoid arthritis; TNF- $\alpha$ , tumor necrosis factor- $\alpha$ .

### CCR7 expression increased in response to inflammatory stimuli in osteoclasts

RA is a chronic inflammatory condition in which tumor necrosis factor- $\alpha$  (TNF- $\alpha$ ) and interleukin-1 $\beta$  (IL-1 $\beta$ ) are constitutively produced. These inflammatory cytokines and LPS were shown to increase the CCL19 and CCL21 mRNA in synovial fibroblasts.<sup>18</sup> As these inflammatory stimuli have a potent impact on RANKL-induced osteoclast differentiation and subsequent bone erosion in the RA synovium, we next investigated whether these factors affected the expression of CCL19 and CCL21 and their receptor CCR7 during osteoclast differentiation from BMMs, the primary cells of osteoclast precursors. The mRNA levels of CCL19 and CCL21 were undetectable during osteoclastic differentiation in the presence and absence of TNF- $\alpha$ , IL-1 $\beta$  or LPS (data not shown).

In contrast to the expression pattern of CCL19 and CCL21, the presence of CCR7 mRNA was clearly detected in BMMs. During RANKL-induced osteoclast differentiation in the absence of inflammatory stimulus, the CCR7 mRNA levels did not change (Figures 2a–c). The addition of TNF- $\alpha$  or IL-1 $\beta$  to cultures containing RANKL increased the CCR7 mRNA by more than four times that of the control (Figures 2a and b), and the addition of LPS increased the CCR7 mRNA by ~15 times that of the control (Figure 2c). Western blotting analyses demonstrated an elevated level of CCR7 protein in the

LPS-stimulated BMMs at 12 and 24 h (Figure 2d). Furthermore, the surface CCR7 level measured at 24 h after LPS stimulation by flow cytometry was higher than that of the PBS-treated group. The addition of LPS increased the surface CCR7 more than 10 times that of the control (Figure 2e). TNF- $\alpha$  and IL-1 $\beta$  also increased the cell surface CCR7 weakly (data not shown). Collectively, TNF- $\alpha$ , IL-1 $\beta$  and LPS increased the expression of CCR7 at the mRNA and protein levels in osteoclast precursors and differentiating cells.

### CCL19 and CCL21 do not affect osteoclast differentiation

We next evaluated the effect of CCL19 and CCL21 on osteoclast differentiation. Precursor BMM cells were cultured with CCL19 in osteoclastogenic medium containing RANKL and subjected to TRAP staining. There was no difference in the number of TRAP-positive multinuclear cells (osteoclasts) between the cytokine-treated group and the untreated group (Figure 3a). Furthermore, no difference was observed between the two groups in terms of the expression of the differentiation marker genes c-Fos, NFATc1 and DC-STAMP (Figure 3b). CCL21 also did not affect the generation of TRAP-positive osteoclasts or the expression of marker genes (Figures 3c and d). Neither CCL19 nor CCL21 induced osteoclast differentiation in the absence of RANKL (data not shown). Therefore, CCL19 and CCL21 did not exert any effect on the formation of osteoclasts.

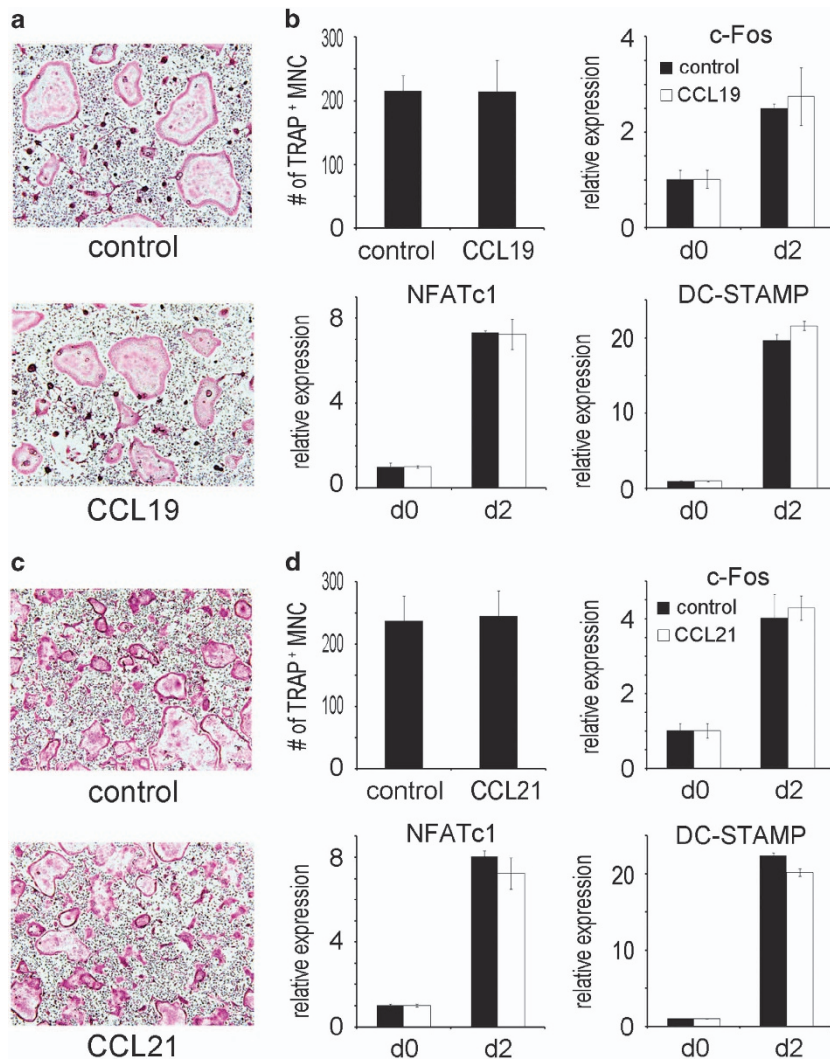


**Figure 3** CCL19 and CCL21 do not affect osteoclast differentiation. (a) BMMs were incubated with M-CSF (30 ng ml<sup>-1</sup>) and RANKL (100 ng ml<sup>-1</sup>) in the absence or presence of CCL19 (10 ng ml<sup>-1</sup>). After 4 days, the cells were fixed with formaldehyde and stained for TRAP. (b) The TRAP-positive multinuclear cells were counted. The mRNA levels of c-Fos, NFATc1 and DCSTAMP were quantified by real-time PCR after 2 days of culture. (c) BMMs were incubated with M-CSF (30 ng ml<sup>-1</sup>) and RANKL (100 ng ml<sup>-1</sup>) with or without CCL21 (10 ng ml<sup>-1</sup>). After 4 days, the cells were fixed with formaldehyde and stained for TRAP. (d) The TRAP-positive multinuclear cells were counted. The mRNA levels for c-Fos, NFATc1 and DCSTAMP were quantified by real-time PCR after 2 days of culture. BMM, bone marrow-derived macrophages.

### CCL19 and CCL21 enhance osteoclast migration

As CCL19 and CCL21 are chemokines that stimulate immune cell migration, we explored the possibility that these chemokines regulate osteoclast migration. We assessed the effect of CCL19 and CCL21 on BMM migration using a transwell system. CCL19 and CCL21 increased the migration of BMMs (Figure 4a). The migration ability of differentiating prefusion osteoclasts was evaluated using the Oris migration assay system. At 16 h after removing the stopper that had blocked cell migration, the stopper areas were filled with more cells in the group treated with CCL19 or CCL21 than the group treated with control vehicle (Figure 4b).

We next investigated whether CCR7 mediated the migration-promoting effect of CCL19 and CCL21. The expression of CCR7 was suppressed by gene knockdown using siRNA

oligonucleotides. The reduction in the CCR7 mRNA and protein was verified by real-time PCR and western blots, respectively (Figure 4c). BMMs with CCR7 knocked down failed to increase migration in response to CCL19 or CCL21 (Figure 4d). These results indicated that CCL19 and CCL21 stimulated the migration of osteoclast precursor cells and differentiating osteoclasts via a CCR7-dependent mechanism.

### CCL19 and CCL21 increase osteoclast resorption activity

We next examined whether CCL19 and CCL21 might have an impact on the resorption function of osteoclasts. BMMs were cultured on calcium phosphate-coated plates in osteoclastogenic medium containing RANKL with or without CCL19 or CCL21. Cells treated with CCL19 or CCL21 generated a greater area of calcium phosphate dissolution than cells not treated

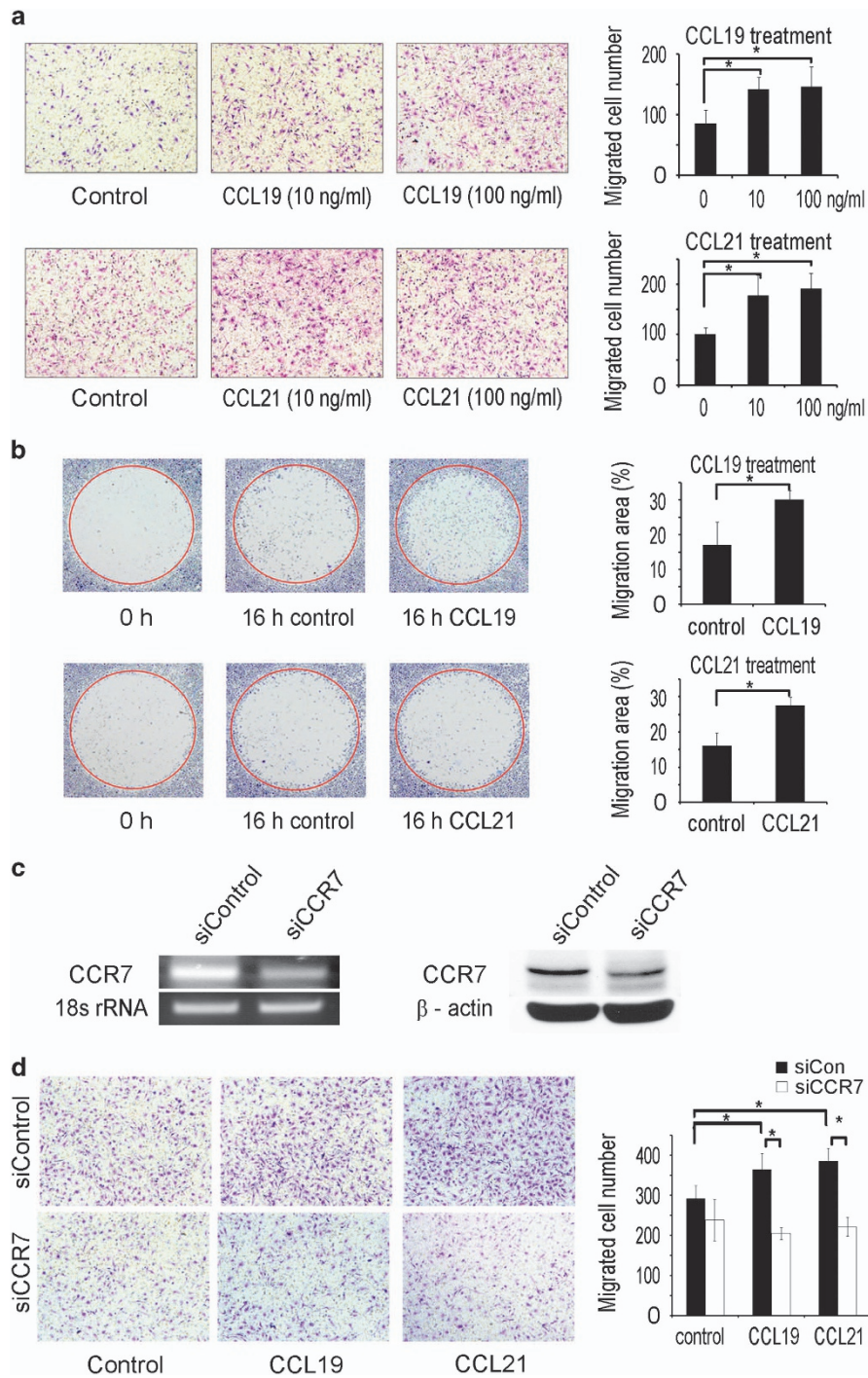


**Figure 4** CCL19 and CCL21 increase the migration of BMMs and osteoclasts. **(a)** BMMs were loaded to the upper chambers of transwell plates. CCL19 or CCL21 were added to the medium in the lower chambers. After 16 h, cells were fixed and stained with crystal violet. The migrated cells were counted. **(b)** BMMs were plated in Oris migration assay plates. The cells were incubated with M-CSF ( $30 \text{ ng ml}^{-1}$ ) and RANKL ( $100 \text{ ng ml}^{-1}$ ). After 2 days, the stoppers were removed, and the cells were washed twice with fresh medium. The cells were incubated with or without CCL19 ( $10 \text{ ng ml}^{-1}$ ) or CCL21 ( $10 \text{ ng ml}^{-1}$ ). After 16 h, the cells were fixed and stained with crystal violet. The stopper areas occupied with cells were quantified. **(c)** BMMs were transfected with control or CCR7 siRNA using Hiperfect. The levels of CCR7 mRNA and protein were assessed by PCR and western blots, respectively. **(d)** BMMs transfected with either CCR7 or control siRNA were loaded into the upper chambers of a transwell plate. CCL19 or CCL21 was added to the lower chambers. After 16 h, the cells were fixed and stained with crystal violet. Migrated BMMs were counted. BMM, bone marrow-derived macrophages; siRNA, small interference RNA.

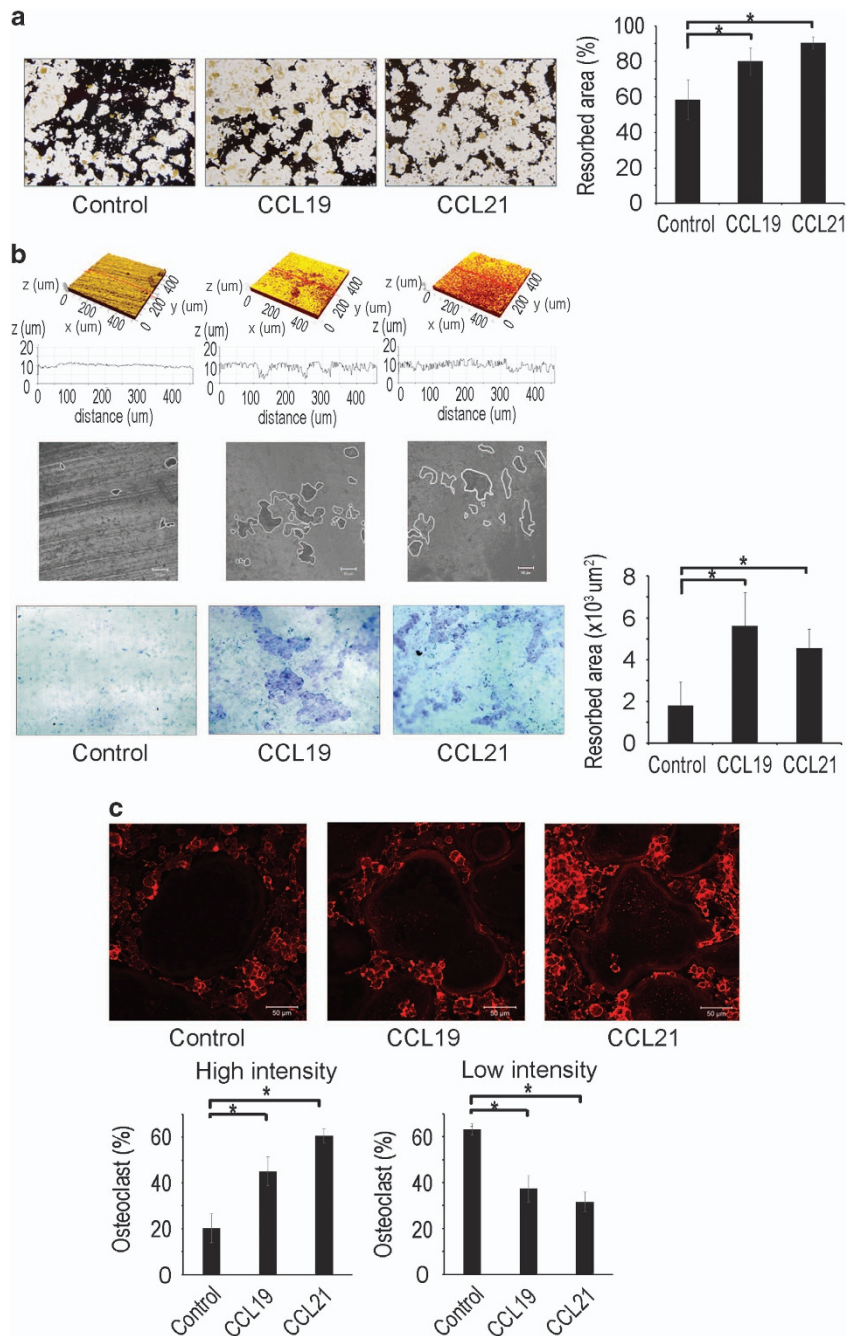


**Figure 5** CCL19 and CCL21 enhance osteoclast bone resorption activity. **(a)** BMMs were placed on calcium phosphate-coated plates and cultured with M-CSF (30 ng ml<sup>-1</sup>) and RANKL (100 ng ml<sup>-1</sup>), along with CCL19 (10 ng ml<sup>-1</sup>) or CCL21 (10 ng ml<sup>-1</sup>). After 6 days, calcium phosphate was stained with von Kossa reagents, and the resorbed area was quantified. **(b)** BMMs were placed on dentin slices and cultured with M-CSF (30 ng ml<sup>-1</sup>) and RANKL (100 ng ml<sup>-1</sup>), along with CCL19 (10 ng ml<sup>-1</sup>) or CCL21 (10 ng ml<sup>-1</sup>). After 6 days, the dentin slice surfaces were analyzed by confocal microscopy. The dentin slices were stained with trypan blue, and the resorption pit areas were quantified. **(c)** BMMs were cultured on cover glasses and cultured with M-CSF (30 ng ml<sup>-1</sup>) and RANKL (100 ng ml<sup>-1</sup>) in the presence of CCL19 (10 ng ml<sup>-1</sup>) or CCL21 (10 ng ml<sup>-1</sup>). After 6 days, the cells were fixed and incubated with rhodamine phalloidin. The actin ring density was quantified by confocal microscopy. BMM, bone marrow-derived macrophages.

with one of these chemokines (Figure 5a). The resorption activity of osteoclasts was also tested with dentine slices. Confocal microscopic analyses revealed that CCL19 and CCL21 increased the number and depth of the resorption pits on dentin surfaces (Figure 5b, top three panels). Quantitative

measurement of the dentine slices after staining with Trypan Blue showed increased resorbed area with CCL19 or CCL21 treatment (Figure 5b, bottom panel). Cytoskeletal rearrangements and actin ring formation are a prerequisite for bone resorption by osteoclasts. To visualize the actin ring

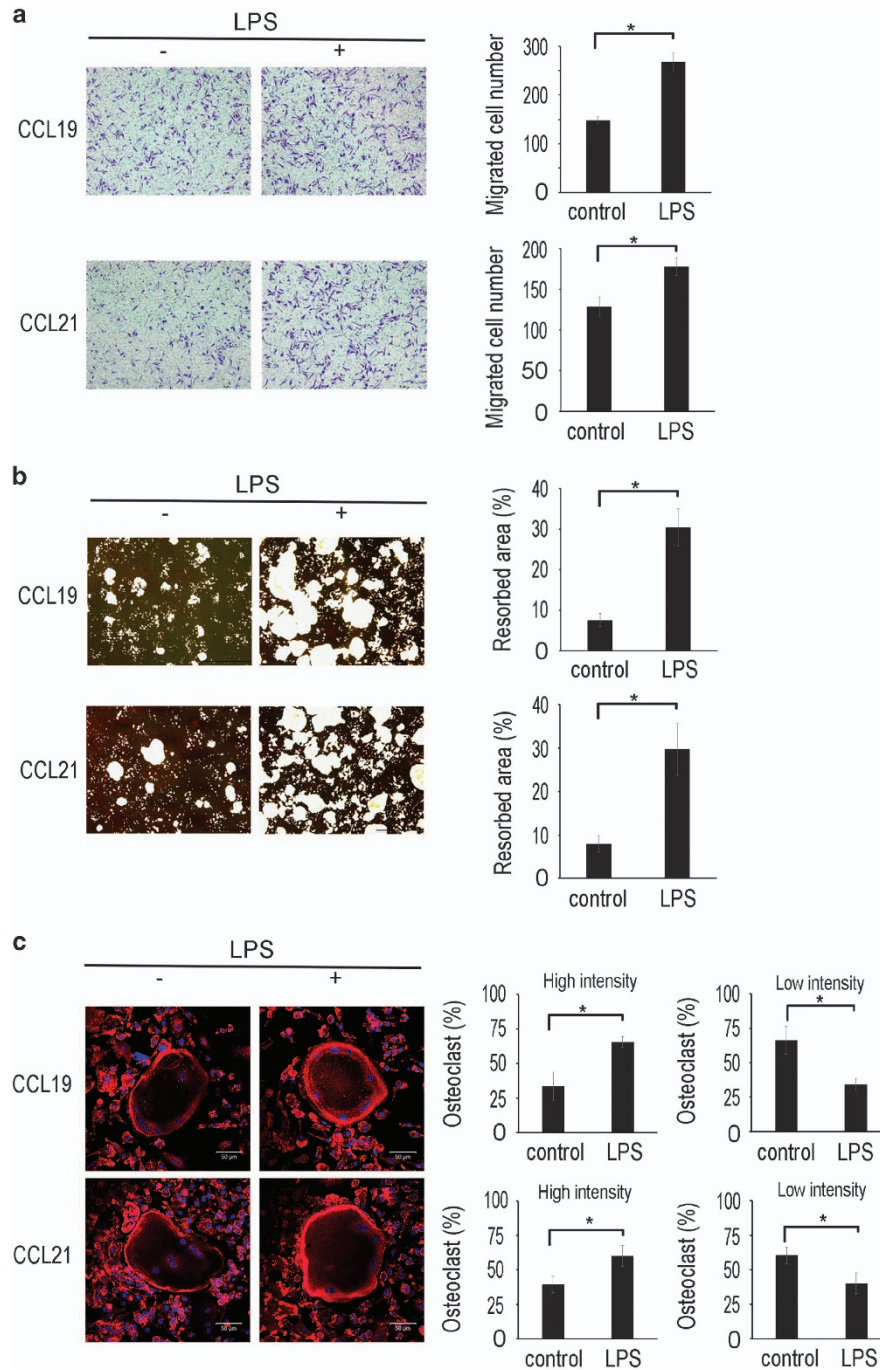


**Figure 6** LPS upregulates the CCL19- and CCL21-induced osteoclast migration and bone resorption activity. **(a)** BMMs were pretreated with LPS ( $5 \text{ ng ml}^{-1}$ ) or control vehicle for 12 h and seeded in the upper chambers of transwell plates. CCL19 ( $10 \text{ ng ml}^{-1}$ ) or CCL21 ( $10 \text{ ng ml}^{-1}$ ) was added to the lower chambers. After 16 h, the cells were fixed and stained with crystal violet. The migrated cells were counted. **(b)** BMMs were seeded on calcium phosphate-coated plates and cultured with M-CSF ( $30 \text{ ng ml}^{-1}$ ) and RANKL ( $100 \text{ ng ml}^{-1}$ ) for 4 days. The cells were pretreated with LPS ( $5 \text{ ng ml}^{-1}$ ) or vehicle. After 1 day, the cells were treated with CCL19 ( $10 \text{ ng ml}^{-1}$ ) or CCL21 ( $10 \text{ ng ml}^{-1}$ ). After 2 days, calcium phosphate was stained with von Kossa reagents, and the resorbed area was quantified. **(c)** BMMs were placed on cover glasses and cultured with M-CSF ( $30 \text{ ng ml}^{-1}$ ) and RANKL ( $100 \text{ ng ml}^{-1}$ ) for 4 days. The cells were treated with CCL19 ( $10 \text{ ng ml}^{-1}$ ) or CCL21 ( $10 \text{ ng ml}^{-1}$ ) after 1 day of pretreatment with LPS ( $5 \text{ ng ml}^{-1}$ ) or control vehicle. At day 6 of the culture, the cells were fixed and incubated with rhodamine phalloidin. The actin ring density was quantified by confocal microscopy. BMM, bone marrow-derived macrophages; LPS, lipopolysaccharide.



formation of osteoclasts, the cells were stained with rhodamine-conjugated phalloidin and subjected to confocal microscopy. Osteoclasts treated with CCL19 or CCL21 showed more dense and prominent actin rings compared with osteoclasts generated in the absence of CCL19 or CCL21 (Figure 5c).

#### LPS enhances CCL19 and CCL21 stimulation of osteoclast migration and bone resorption activity

We next evaluated the effects of CCR7 upregulation on the stimulatory function of CCL19 and CCL21 on osteoclast migration, bone resorption and actin ring formation. To this end, the cells were pretreated with LPS to induce CCR7 expression before stimulation with CCL19 or CCL21. LPS pretreatment increased the migration of BMMs induced by CCL19 or CCL21 in the transwell assays (Figure 6a). In addition, LPS augmented the positive effect of CCL19 and CCL21 on the resorption activity of osteoclasts on calcium phosphate-coated plates (Figure 6b). Consistently, osteoclasts treated with LPS generated more prominent actin rings than the cells in the control group (Figure 6c). These data suggested that LPS, probably via CCR7 upregulation, further increases osteoclast migration, bone resorption activity and actin ring formation in response to CCL19 or CCL21.

#### CCL19 and CCL21 stimulate osteoclasts via the Rho-ROCK signaling pathway

Active RhoA GTPase is crucial for cell migration, and CCR7 activates RhoA GTPase in monocytes.<sup>20</sup> Therefore, we investigated the involvement of RhoA in the CCL19 and CCL21 stimulation of osteoclasts. In pull-down experiments to precipitate active RhoA protein, both CCL19 and CCL21 activated RhoA within 15 min (Figure 7a). ROCK is a major downstream target of activated RhoA.<sup>26</sup> To evaluate the ROCK activity, phosphorylated myosin light chain (p-MLC) was measured using western blots. The p-MLC levels increased after 15 min of stimulation with CCL19 or CCL21 (Figure 7b). To gain further support for the involvement of Rho activation in osteoclast migration, the Rho inhibitors simvastatin and Y27632 were added to the transwell assays. Both Rho inhibitors did not affect BMM viability up to 10  $\mu$ M (data not shown). The cells treated with Rho inhibitors had a lower migratory response to CCL19 and CCL21 than the cells treated with vehicle (Figure 7c). When Rho inhibitors were added to the cells cultured on calcium-phosphate plates, the resorption activity of the osteoclasts was significantly suppressed (Figure 7d). Taken together, these results suggested that the Rho-ROCK signaling pathway mediates the effect of CCL19 and CCL21 on the migration and resorption activities of osteoclasts.

#### CCL19 and CCL21 increase mouse calvarial bone resorption

To gain evidence for the *in vivo* effects of CCL19 and CCL21 on bone resorption, we utilized a mouse calvarial model. Chemokine-soaked collagen sheets were transplanted into mouse calvariae, and  $\mu$ -CT and histomorphometric

analyses were performed 7 days after transplantation. CCL19-treated calvariae showed a significantly more resorbed area compared to the PBS-treated calvariae. The PBS-treated group showed 1.79-times more bone volume than that of the CCL19-treated group (Figure 8a). Histologic analyses revealed that the CCL19-treated group had a greater osteoclast surface/bone surface (Figure 8a). Since LPS and inflammatory cytokines increased the CCR7 expression, the response to CCL19 or CCL21 might be augmented under inflammatory conditions. To test this possibility, we injected LPS into mice intraperitoneally 1 day before the transplantation of CCL19-soaked collagen. Under these conditions, CCL19 further increased bone resorption and the osteoclast surface/bone surface (Figure 8a). The bone volume of the PBS-treated group was 2.55 times higher than that of the CCL19-treated group (Figure 8a). CCL21 also increased resorption in the calvariae: the bone volume of the PBS-treated group was 1.35 times higher than that of the CCL21-treated group and had a greater osteoclast surface/bone surface value (Figure 8b). An increased osteoclast surface/bone surface was also observed in the CCL21-treated mice (Figure 8b). These *in vivo* results provide further evidence for the stimulatory function of CCL19 and CCL21 on osteoclast migration and bone resorption.

#### DISCUSSION

There is accumulating evidence for an association between the chemokines CCL19 and CCL21 and RA. Using immunohistochemistry, the expression of CCL19 and CCL21 was shown to be higher in synovial tissues from RA patients than in normal tissues.<sup>18</sup> Our analysis of a cDNA microarray data set (GSE1919) revealed higher mRNA levels of CCL19 and CCL21 in RA synovial tissues than in normal synovial tissues (Supplementary Figure 1), supporting the immunohistochemical results. A previous study using an ELISA to examine the levels of CCL19 and CCL21 in synovial fluids also found increased levels of CCL19 and CCL21 in RA patients compared to those in OA patients.<sup>18</sup> Our experiments confirmed the elevated levels of those cytokines in RA synovial fluids and further detected elevation in the serum (Figure 1). In addition, genome-wide association studies have implicated the CCL21 locus as a RA susceptibility gene.<sup>27,28</sup> These findings suggest the possibility of using CCL19 or CCL21 as biochemical indicators for diagnosing and monitoring the treatment of RA. In support of this proposition, the level of CCL19 in RA patients falls below that of the control level after 1 year of treatment.<sup>19</sup>

Some studies suggest that CCR7 is involved in the angiogenesis and migration of leukocytes and lymphocytes to the synovium in RA.<sup>29-31</sup> Using immunostaining, it was found that the CCR7 protein is more abundant in RA synovial tissues than in normal tissues.<sup>31</sup> In concordance with this report, our analyses of the microarray data set GSE1919 revealed more CCR7 in the synovial tissues from RA patients than in tissues from normal controls (Supplementary Figure 2a). The results using another data set, GSE10500, showed that among nine CCR family receptors, CCR7 was selectively upregulated on

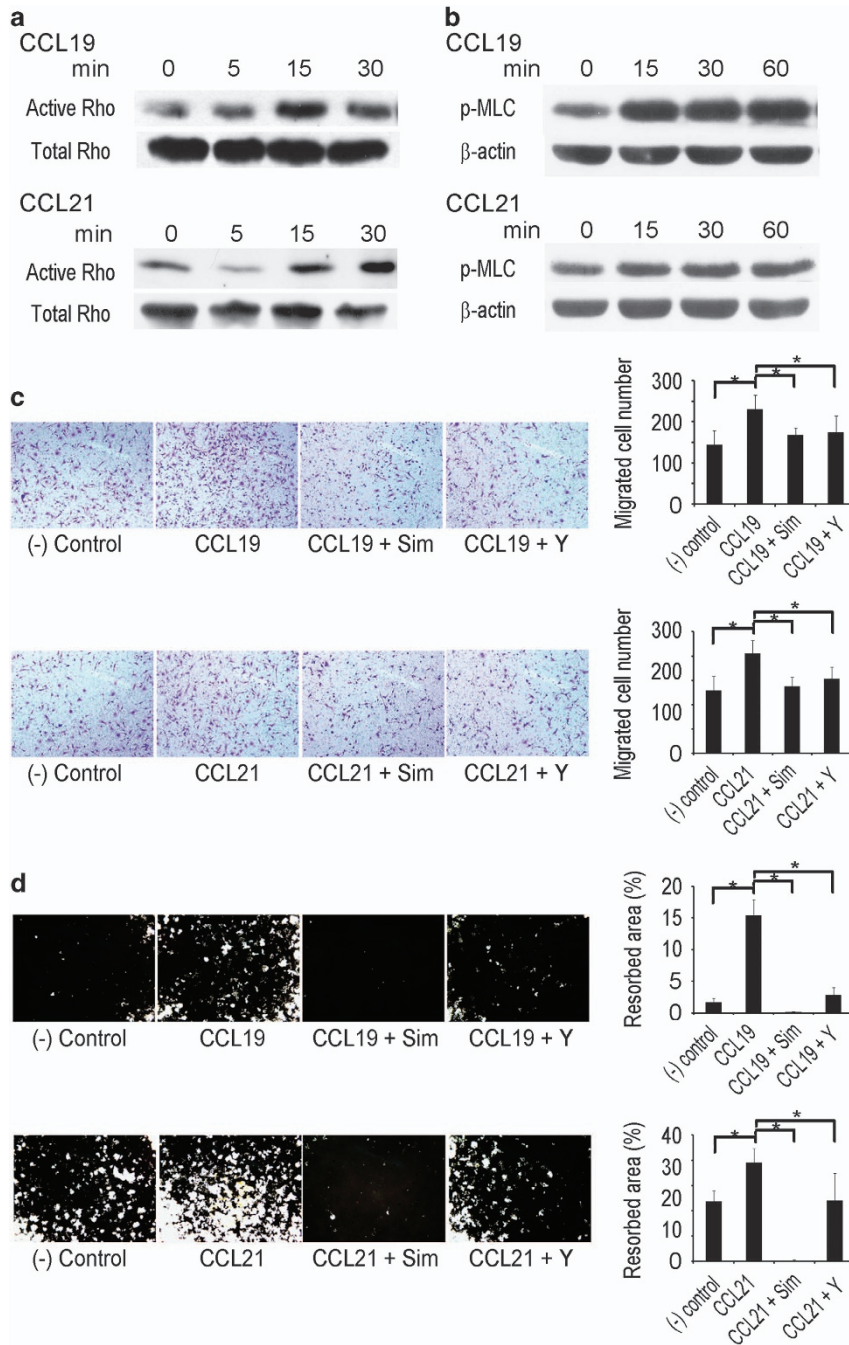


**Figure 7** CCL19 and CCL21 activate osteoclast migration and resorption through Rho signaling. **(a)** BMMs were cultured with M-CSF ( $30 \text{ ng ml}^{-1}$ ) for 2 days. After serum starvation for 6 h, the cells were treated with CCL19 ( $10 \text{ ng ml}^{-1}$ ) or CCL21 ( $10 \text{ ng ml}^{-1}$ ) for 0, 5, 15 and 30 min. The cells were lysed, and GTP-bound active Rho was pulled down for western blots. A portion of the cell lysate was used to detect the total RhoA protein. **(b)** BMMs were cultured with M-CSF ( $30 \text{ ng ml}^{-1}$ ) for 2 days. After 6 h serum starvation, the cells were stimulated with CCL19 ( $10 \text{ ng ml}^{-1}$ ) or CCL21 ( $10 \text{ ng ml}^{-1}$ ). PMLC in the cell lysates was measured by western blots.  $\beta$ -Actin was used as a loading control. **(c)** BMMs were pretreated with Rho inhibitors (simvastatin and Y27632) for 1 h and loaded into the upper chambers of a transwell plate. CCL19 ( $10 \text{ ng ml}^{-1}$ ) or CCL21 ( $10 \text{ ng ml}^{-1}$ ) was added to the bottom chamber. After 16 h, the cells were fixed and stained with crystal violet. **(d)** BMMs were seeded and cultured with M-CSF ( $30 \text{ ng ml}^{-1}$ ) and RANKL ( $100 \text{ ng ml}^{-1}$ ) on calcium phosphate-coated plates. After 4 days, the cells were treated with Rho inhibitors (simvastatin and Y27632) in addition to CCL19 ( $10 \text{ ng ml}^{-1}$ ) or CCL21 ( $10 \text{ ng ml}^{-1}$ ). After 2 days, the cells were removed, and calcium phosphate was stained using the von Kossa method. The resorbed area was quantified. BMM, bone marrow-derived macrophage.

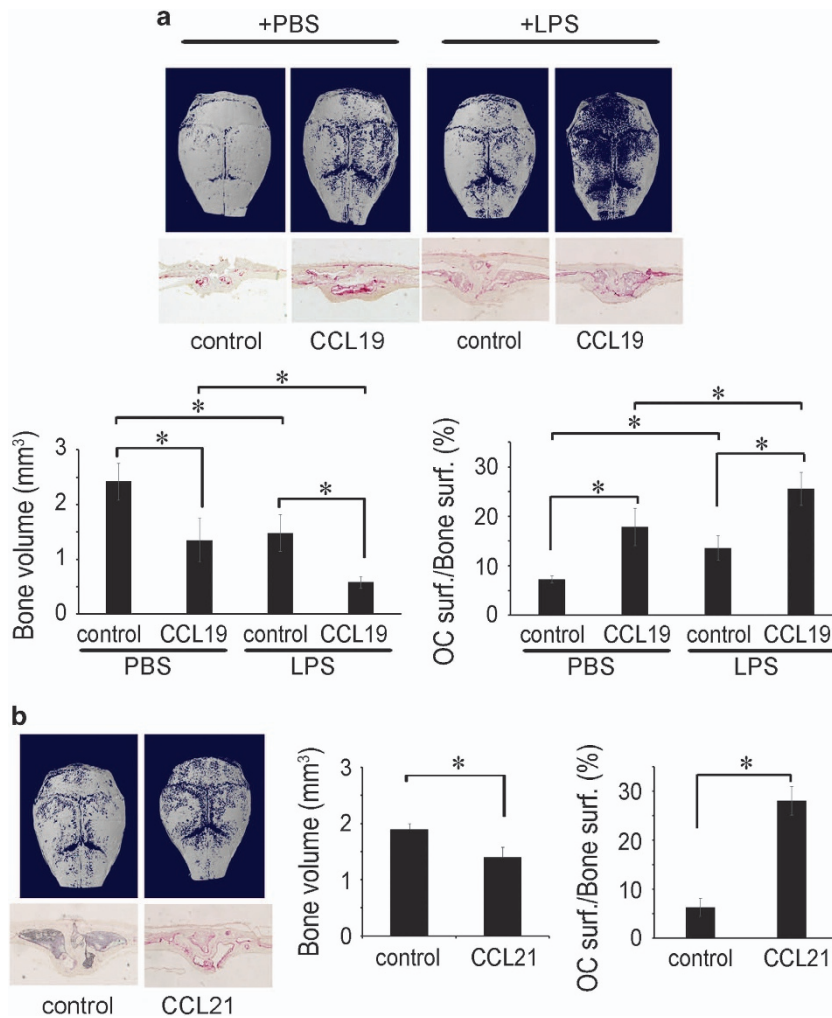


**Figure 8** CCL19 and CCL21 stimulate bone resorption *in vivo*. **(a)** Collagen sponges soaked with CCL19 (2  $\mu$ g) or PBS were transplanted into 5-week-old ICR mouse calvariae. LPS or PBS was injected into the mice intraperitoneally 1 day before and 3 days after transplantation. At 7 days after transplantation, the calvariae were fixed with 4% paraformaldehyde and analyzed by  $\mu$ -CT. The decalcified calvarial tissue sections were stained for TRAP, and the osteoclast surface/bone surface index was assessed using the Osteomeasure program. **(b)** Collagen sponges soaked with CCL21 (2  $\mu$ g) or PBS were transplanted into 5-week-old ICR mouse calvariae. After 7 days, the calvariae were fixed with 4% paraformaldehyde for 1 day and analyzed by  $\mu$ -CT. The osteoclast surface/bone surface index was determined with decalcified calvarial sections after TRAP-staining using the Osteomeasure program. LPS, lipopolysaccharide;  $\mu$ -CT, micro-computed tomography.

synovial macrophages from RA patients (Supplementary Figure 2b). Therefore, compared to other CCR types, the CCR7 isoform may have a distinct function as a crucial mediator of RA pathogenesis. In support of this hypothesis, elevated CCR7 on circulating monocytes and T-cells was reduced to baseline by methotrexate treatment in early RA patients.<sup>19</sup> However, the molecular mechanisms and the type of cells that are key elements in the contribution of CCR7 to RA pathogenesis require further investigation.

Monocytes and macrophages are precursor cells that can differentiate into osteoclasts. In our study, CCR7 expression in BMMs was upregulated by treatment with TNF- $\alpha$ , IL-1 $\beta$  and LPS (Figure 2), while the expression of CCL19 and CCL21 was not detected in BMMs and osteoclasts under challenge or nonchallenge conditions (data not shown). However,

inflammatory stimuli increase the CCL19 and CCL21 levels in macrophages and synovial fibroblasts from RA patients.<sup>18</sup> Therefore, TNF- $\alpha$  and IL-1 $\beta$ , which are frequently elevated in RA, may potentiate the recruitment of osteoclast precursor cells to the inflammatory sites of RA via the upregulation of the CCR7 receptor and CCL19/CCL21 ligand pairs. Our experiments with an *in vivo* calvarial bone lysis model showed more bone loss in response to CCL19 in mice treated with LPS (Figure 8). This result supports a positive *in vivo* role for CCR7 in the recruitment of osteoclast precursor cells and subsequent bone resorption. Consistently, LPS pretreatment enhanced the stimulatory effects of CCL19 and CCL21 on cell migration and bone resorption *in vitro* (Figure 6). The osteoclast differentiation factor RANKL alone, without other inflammatory stimuli, had no effect on the CCR7 levels (Figures 2a–c). This result

implies that CCR7 and its ligands have little effect on normal bone remodeling; rather, they have significant impact on bone lysis under inflammatory conditions, such as RA. Therefore, therapeutic strategies targeting CCR7 may have an advantage over other osteoclast-suppressing agents in blocking bone destruction in RA patients.

In spite of extensive studies on the migration-promoting roles of CCL19 and CCL21 in immune responses,<sup>32–37</sup> the effects of CCL19 and CCL21 on osteoclast function have not been studied to date. Other migration-regulating cytokines, such as SDF-1, TGF $\beta$ , CX<sub>3</sub>CL1 and macrophage migration inhibitory factor, affect osteoclastogenesis directly or indirectly.<sup>3–5,38,39</sup> Unlike these cytokines, CCL19 and CCL21 had no effect on osteoclast formation; rather, they promoted the migration and resorption activity of BMMs and osteoclasts (Figures 3,4,5). In the *in vivo* calvarial model, the CCL19- and CCL21-treated groups showed higher osteoclast surface/bone surface values than the control groups (Figure 8). This *in vivo* result of seemingly increased osteoclastogenesis is likely to be due to the stimulatory effect of the cytokines on the migration of osteoclast precursor cells rather than an effect on differentiation *per se*. The migration and resorption responses involve actin cytoskeletal events. The activation of the small GTPase RhoA is a critical step in actin cytoskeleton reorganization. Previous studies have shown that RhoA is responsible for osteoclast motility,<sup>24</sup> podosome organization,<sup>40</sup> actin ring and sealing zone formation,<sup>41</sup> and bone resorption.<sup>24</sup> Downstream of RhoA, ROCK activates WASP, myosin light chain and ERM proteins,<sup>42,43</sup> which are implicated in bone resorption.<sup>44,45</sup> In this study, we found that the stimulation of osteoclast migration, actin ring formation and bone resorption by CCL19 and CCL21 was mediated by the Rho–ROCK pathway.

In summary, we found that the levels of the chemokines CCL19 and CCL21 were elevated in the blood and synovial fluids of RA patients. The expression of the CCL19 and CCL21 receptor CCR7 was also markedly increased in the synovial tissues of RA patients. In addition, CCR7 was upregulated in osteoclasts by inflammatory stimuli. CCL19 and CCL21 stimulated osteoclast migration and resorption activity via the CCR7/Rho signaling pathway. Our findings support the CCL19/CCL21–CCR7 interaction as a novel focus in the development of RA therapeutics. Neutralizing antibodies for the chemokines and CCR7-reducing strategies involving CCR7 monoclonal antibodies,<sup>46</sup> histone H3K27me3 methylation,<sup>47</sup> and miRNA 7a and miRNA 21<sup>48,49</sup> may be explored to reduce both lymphocyte infiltration and osteoclastic bone resorption to effectively alleviate RA progression.

## CONFLICT OF INTEREST

The authors declare no conflict of interest.

## ACKNOWLEDGEMENTS

This work was supported by a grant from the National Research Foundation of Korea (NRF-2014R1A2A1A10050406) to H-HK

*Author contributions:* All authors were involved in drafting the article and revising it critically for important intellectual content, and all authors approved the final version to be published. H-HK had full access to all the data and takes responsibility for the integrity of the data and accuracy of the data analysis. Study conception and design: JL, ZHL, YWS and H-HK. Acquisition of data: JL, CP and YDL. Analysis and interpretation of data: JL, HJK and H-HK.

- 1 Sharp JT, Wolfe F, Mitchell DM, Bloch DA. The progression of erosion and joint space narrowing scores in rheumatoid arthritis during the first twenty-five years of disease. *Arthritis Rheum* 1991; **34**: 660–668.
- 2 Mulherin D, Fitzgerald O, Bresnihan B. Synovial tissue macrophage populations and articular damage in rheumatoid arthritis. *Arthritis Rheum* 1996; **39**: 115–124.
- 3 Yu X, Huang Y, Collin-Osdoby P, Osdoby P. Stromal cell-derived factor-1 (SDF-1) recruits osteoclast precursors by inducing chemotaxis, matrix metalloproteinase-9 (MMP-9) activity, and collagen transmigration. *J Bone Miner Res* 2003; **18**: 1404–1418.
- 4 Pilkington MF, Sims SM, Dixon SJ. Transforming growth factor-beta induces osteoclast ruffling and chemotaxis: potential role in osteoclast recruitment. *J Bone Miner Res* 2001; **16**: 1237–1247.
- 5 Koizumi K, Saitoh Y, Minami T, Takeno N, Tsuneyama K, Miyahara T et al. Role of CX3CL1/fractalkine in osteoclast differentiation and bone resorption. *J Immunol* 2009; **183**: 7825–7831.
- 6 Seth S, Oberdorfer L, Hyde R, Hoff K, Thies V, Worbs T et al. CCR7 essentially contributes to the homing of plasmacytoid dendritic cells to lymph nodes under steady-state as well as inflammatory conditions. *J Immunol* 2011; **186**: 3364–3372.
- 7 Beauvillain C, Cunin P, Doni A, Scotet M, Jaillon S, Loiry ML et al. CCR7 is involved in the migration of neutrophils to lymph nodes. *Blood* 2011; **117**: 1196–1204.
- 8 Ueno T, Hara K, Willis MS, Malin MA, Hopken UE, Gray DH et al. Role for CCR7 ligands in the emigration of newly generated T lymphocytes from the neonatal thymus. *Immunity* 2002; **16**: 205–218.
- 9 Cabioglu N, Yazici MS, Arun B, Broglio KR, Hortobagyi GN, Price JE et al. CCR7 and CXCR4 as novel biomarkers predicting axillary lymph node metastasis in T1 breast cancer. *Clin Cancer Res* 2005; **11**: 5686–5693.
- 10 Koizumi K, Kozawa Y, Ohashi Y, Nakamura ES, Aozuka Y, Sakurai H et al. CCL21 promotes the migration and adhesion of highly lymph node metastatic human non-small cell lung cancer Lu-99 *in vitro*. *Oncol Rep* 2007; **17**: 1511–1516.
- 11 Peng C, Zhou K, An S, Yang J. The effect of CCL19/CCR7 on the proliferation and migration of cell in prostate cancer. *Tumour Biol* 2015; **36**: 329–335.
- 12 Scandella E, Men Y, Gillessen S, Forster R, Groettrup M. Prostaglandin E2 is a key factor for CCR7 surface expression and migration of monocyte-derived dendritic cells. *Blood* 2002; **100**: 1354–1361.
- 13 Britschgi MR, Favre S, Luther SA. CCL21 is sufficient to mediate DC migration, maturation and function in the absence of CCL19. *Eur J Immunol* 2010; **40**: 1266–1271.
- 14 Forster R, Schubel A, Breitfeld D, Kremmer E, Renner-Muller I, Wolf E et al. CCR7 coordinates the primary immune response by establishing functional microenvironments in secondary lymphoid organs. *Cell* 1999; **99**: 23–33.
- 15 Ato M, Nakano H, Kakiuchi T, Kaye PM. Localization of marginal zone macrophages is regulated by C-C chemokine ligands 21/19. *J Immunol* 2004; **173**: 4815–4820.
- 16 Comerford I, Harata-Lee Y, Bunting MD, Gregor C, Kara EE, McCol SR. A myriad of functions and complex regulation of the CCR7/CCL19/CCL21 chemokine axis in the adaptive immune system. *Cytokine Growth Factor Rev* 2013; **24**: 269–283.
- 17 Zhang W, Tu G, Lv C, Long J, Cong L, Han Y. Matrix metalloproteinase-9 is up-regulated by CCL19/CCR7 interaction via PI3K/Akt pathway and is involved in CCL19-driven BMSCs migration. *Biochem Biophys Res Commun* 2014; **451**: 222–228.
- 18 Pickens SR, Chamberlain ND, Volin MV, Pope RM, Mandelin AM 2nd, Shahrara S. Characterization of CCL19 and CCL21 in rheumatoid arthritis. *Arthritis Rheum* 2011; **63**: 914–922.
- 19 Ellingsen T, Hansen I, Thorsen J, Moller BK, Tarp U, Lottenburger T et al. Upregulated baseline plasma CCL19 and CCR7 cell-surface expression on

- monocytes in early rheumatoid arthritis normalized during treatment and CCL19 correlated with radiographic progression. *Scand J Rheumatol* 2014; **43**: 91–100.
- 20 Allaire MA, Dumais N. Involvement of the MAPK and RhoA/ROCK pathways in PGE2-mediated CCR7-dependent monocyte migration. *Immunol Lett* 2012; **146**: 70–73.
- 21 Bardi G, Niggli V, Loetscher P. Rho kinase is required for CCR7-mediated polarization and chemotaxis of T lymphocytes. *FEBS Lett* 2003; **542**: 79–83.
- 22 Fukuda A, Hikita A, Wakeyama H, Akiyama T, Oda H, Nakamura K *et al*. Regulation of osteoclast apoptosis and motility by small GTPase binding protein Rac1. *J Bone Miner Res* 2005; **20**: 2245–2253.
- 23 Ito Y, Teitelbaum SL, Zou W, Zheng Y, Johnson JF, Chappel J *et al*. Cdc42 regulates bone modeling and remodeling in mice by modulating RANKL/M-CSF signaling and osteoclast polarization. *J Clin Invest* 2010; **120**: 1981–1993.
- 24 Chellaiah MA, Soga N, Swanson S, McAllister S, Alvarez U, Wang D *et al*. Rho-A is critical for osteoclast podosome organization, motility, and bone resorption. *J Biol Chem* 2000; **275**: 11993–12002.
- 25 Chang EJ, Ha J, Oerlemans F, Lee YJ, Lee SW, Ryu J *et al*. Brain-type creatine kinase has a crucial role in osteoclast-mediated bone resorption. *Nat Med* 2008; **14**: 966–972.
- 26 Hanna S, El-Sibai M. Signaling networks of Rho GTPases in cell motility. *Cell Signal* 2013; **25**: 1955–1961.
- 27 Freudenberg J, Lee HS, Han BG, Shin HD, Kang YM, Sung YK *et al*. Genome-wide association study of rheumatoid arthritis in Koreans: population-specific loci as well as overlap with European susceptibility loci. *Arthritis Rheum* 2011; **63**: 884–893.
- 28 Stahl EA, Raychaudhuri S, Remmers EF, Xie G, Eyre S, Thomson BP *et al*. Genome-wide association study meta-analysis identifies seven new rheumatoid arthritis risk loci. *Nat Genet* 2010; **42**: 508–514.
- 29 Page G, Lebecque S, Miossec P. Anatomic localization of immature and mature dendritic cells in an ectopic lymphoid organ: correlation with selective chemokine expression in rheumatoid synovium. *J Immunol* 2002; **168**: 5333–5341.
- 30 Nanki T, Takada K, Komano Y, Morio T, Kanegane H, Nakajima A *et al*. Chemokine receptor expression and functional effects of chemokines on B cells: implication in the pathogenesis of rheumatoid arthritis. *Arthritis Res Ther* 2009; **11**: R149.
- 31 Pickens SR, Chamberlain ND, Volin MV, Pope RM, Talarico NE, Mandelin AM 2nd *et al*. Role of the CCL21 and CCR7 pathways in rheumatoid arthritis angiogenesis. *Arthritis Rheum* 2012; **64**: 2471–2481.
- 32 Cote SC, Pasvanis S, Bounou S, Dumais N. CCR7-specific migration to CCL19 and CCL21 is induced by PGE(2) stimulation in human monocytes: Involvement of EP(2)/EP(4) receptors activation. *Mol Immunol* 2009; **46**: 2682–2693.
- 33 Randolph GJ. Dendritic cell migration to lymph nodes: cytokines, chemokines, and lipid mediators. *Semin Immunol* 2001; **13**: 267–274.
- 34 Randolph GJ, Ochoa J, Partida-Sanchez S. Migration of dendritic cell subsets and their precursors. *Annu Rev Immunol* 2008; **26**: 293–316.
- 35 Reif K, Ekland EH, Ohl L, Nakano H, Lipp M, Forster R *et al*. Balanced responsiveness to chemoattractants from adjacent zones determines B-cell position. *Nature* 2002; **416**: 94–99.
- 36 Sallusto F, Lenig D, Forster R, Lipp M, Lanzavecchia A. Two subsets of memory T lymphocytes with distinct homing potentials and effector functions. *Nature* 1999; **401**: 708–712.
- 37 Szanya V, Ermann J, Taylor C, Holness C, Fathman CG. The subpopulation of CD4+CD25+ splenocytes that delays adoptive transfer of diabetes expresses L-selectin and high levels of CCR7. *J Immunol* 2002; **169**: 2461–2465.
- 38 Ruan M, Pederson L, Bradley EW, Bamberger AM, Oursler MJ. Transforming growth factor- $\beta$  coordinately induces suppressor of cytokine signaling 3 and leukemia inhibitory factor to suppress osteoclast apoptosis. *Endocrinology* 2010; **151**: 1713–1722.
- 39 Jacquin C, Koczon-Jaremko B, Aguila HL, Leng L, Bucala R, Kuchel GA *et al*. Macrophage migration inhibitory factor inhibits osteoclastogenesis. *Bone* 2009; **45**: 640–649.
- 40 Chellaiah MA. Regulation of podosomes by integrin  $\alpha$ v $\beta$ 3 and Rho GTPase-facilitated phosphoinositide signaling. *Eur J Cell Biol* 2006; **85**: 311–317.
- 41 Kikuta J, Ishii M. Osteoclast migration, differentiation and function: novel therapeutic targets for rheumatic diseases. *Rheumatology* 2013; **52**: 226–234.
- 42 Julian L, Olson MF. Rho-associated coiled-coil containing kinases (ROCK): structure, regulation, and functions. *Small GTPases* 2014; **5**: e29846.
- 43 Matsui T, Maeda M, Doi Y, Yonemura S, Amano M, Kaibuchi K *et al*. Rho-kinase phosphorylates COOH-terminal threonines of ezrin/radixin/moesin (ERM) proteins and regulates their head-to-tail association. *J Cell Biol* 1998; **140**: 647–657.
- 44 Chellaiah MA, Biswas RS, Rittling SR, Denhardt DT, Hruska KA. Rho-dependent Rho kinase activation increases CD44 surface expression and bone resorption in osteoclasts. *J Biol Chem* 2003; **278**: 29086–29097.
- 45 Chellaiah MA, Kuppaswamy D, Lasky L, Linder S. Phosphorylation of a Wiscott-Aldrich syndrome protein-associated signal complex is critical in osteoclast bone resorption. *J Biol Chem* 2007; **282**: 10104–10116.
- 46 Somovilla-Crespo B, Alfonso-Perez M, Cuesta-Mateos C, Carballo-de Dios C, Beltran AE, Terron F *et al*. Anti-CCR7 therapy exerts a potent anti-tumor activity in a xenograft model of human mantle cell lymphoma. *J Hematol Oncol* 2013; **6**: 89.
- 47 Moran TP, Nakano H, Kondilis-Mangum HD, Wade PA, Cook DN. Epigenetic control of Ccr7 expression in distinct lineages of lung dendritic cells. *J Immunol* 2014; **193**: 4904–4913.
- 48 Kim SJ, Shin JY, Lee KD, Bae YK, Sung KW, Nam SJ *et al*. MicroRNA let-7a suppresses breast cancer cell migration and invasion through downregulation of C-C chemokine receptor type 7. *Breast Cancer Res* 2012; **14**: R14.
- 49 Smigielska-Czepiel K, van den Berg A, Jellema P, Slezak-Prochazka I, Maat H, van den Bos H *et al*. Dual role of miR-21 in CD4+ T-cells: activation-induced miR-21 supports survival of memory T-cells and regulates CCR7 expression in naive T-cells. *PLoS ONE* 2013; **8**: e76217.



This work is licensed under a Creative Commons Attribution-NonCommercial-NoDerivs 4.0 International License. The images or other third party material in this article are included in the article's Creative Commons license, unless indicated otherwise in the credit line; if the material is not included under the Creative Commons license, users will need to obtain permission from the license holder to reproduce the material. To view a copy of this license, visit <http://creativecommons.org/licenses/by-nc-nd/4.0/>

Supplementary Information accompanies the paper on Experimental & Molecular Medicine website (<http://www.nature.com/emm>)